

Vol. 3, No. 2 February 2009

A Novel Method of Image Compression

Using Multiwavelets and Set Partitioning Algorithm

U.S.Ragupathy (Corresponding author) Department of EEE Kongu Engineering College Perundurai, Erode – 638 052 Tamil Nadu, India E-mail: ragupathy_us@yahoo.co.in

A.Tamilarasi Department of MCA Kongu Engineering College Perundurai, Erode – 638 052 Tamil Nadu, India E-mail: a_tamilarasi@kongu.ac.in

Abstract

Advances in wavelet transforms and quantization methods have produced algorithms capable of surpassing the existing image compression standards like the Joint Photographic Experts Group (JPEG) algorithm. The existing compression methods for JPEG standards are using DCT with arithmetic coding and DWT with Huffman coding. The DCT uses a single kernel where as wavelet offers more number of filters depends on the applications. The wavelet based Set Partitioning In Hierarchical Trees (SPIHT) algorithm gives better compression. For best performance in image compression, wavelet transforms require filters that combine a number of desirable properties, such as orthogonality and symmetry, but they cannot simultaneously possess all of these properties. The relatively new field of multiwavelets offer more design options and can combine all desirable transform features. But there are some limitations in using the SPIHT algorithm for multiwavelets coefficients. This paper presents a new method for encoding the multiwavelet decomposed images by defining coefficients suitable for SPIHT algorithm which gives better compression performance over the existing methods in many cases.

Keywords: Wavelets, Multiwavelets, Decomposition, SPIHT

1. Introduction

A number of methods have been presented over the years to perform image compression. However the goal is unique to alter the representation of information contained in an image so that it can be represented sufficiently well with less information. Current methods for lossless image compression typically use some form of Huffman or arithmetic coder (Ian H. Witten, Radford M. Neal, and John G. Cleary. 1987.) or an integer-to-integer wavelet transform (R. C. Calderbank, Ingrid Daubechies, Wim Sweldens, and Boon-Lock Yeo. 1998.). To achieve a high compression factor, a lossy method must be used. The most popular current lossy image compression methods use a transform based scheme.

The JPEG standard uses DCT with run-length coding of 0's and Huffman or arithmetic coding. The JPEG 2000 standard (ISO/IEC IS 15444-1 / ITU-T Rec. T.800) uses wavelet analysis with EBCOT bitplane encoding and arithmetic coding (Zixiang Xiong, Michael T. Orchard, and Kannan Ramchandran. 1997.). Wavelet transforms allow additional freedom in the selection of the particular wavelet filter used; in contrast, there is only one DCT filter. And also the wavelet filters can be chosen depending on the images and applications.

Both wavelet theory and methods for its application to image compression have been well developed over the past decade. JPEG2000 uses wavelet filters with different properties like orthogonal, symmetric and biorthogonal etc. It

mainly uses the Daubechies filters (Ingrid Daubechies. 1992.)(Michael Unser, Thierry Blu. 2003.). Daubechies wavelets are orthogonal and have compact support, but they do not have a closed analytic form and the lowest order families do not have continuous derivatives everywhere. All these wavelets are called as scalar wavelets since they have only one scaling and one wavelet function. In most cases, the scalar wavelets are failed to satisfy the orthogonal, symmetric, anti symmetric and biorthogonal properties simultaneously (V. Strela, P. N. Heller, G. Strang, P. Topiwala, and C. Heil. 1998.) (V. Strela. 1997.). This can be fulfilled by the use of multiwavelets which has more than one scaling and wavelet functions. Much of the current theory of multiwavelets comes from Vasily Strela (V. Strela and A. T. Walden. 1998.) (V. Strela, P. N. Heller, G. Strang, P. Topiwala, and C. Heil. 1998.) (V. Strela, P. N. Heller, G. Strang, P. Topiwala, and C. Heil. 1998.) (V. Strela, P. N. Heller, G. Strang, P. Topiwala, and C. Heil. 1998.) (V. Strela, P. N. Heller, G. Strang, P. Topiwala, and Wavelet functions. Much of the current theory of multiwavelets comes from Vasily Strela (V. Strela and A. T. Walden. 1998.) (V. Strela, P. N. Heller, G. Strang, P. Topiwala, and C. Heil. 1998.) (V. Strela, 1995.) and the members of the Wavelets Strategic Research Programme (WSRP) at the National University of Singapore.

Recent literature on the subject of multiwavelets has focused mostly on development of the basic theory (Jo Yew Tham, Li-Xin Shen, Seng Luan Lee, and Hwee Huat Tan. 1998.)(V. Strela. 1996.)(Tao Xia and Qingtang Jiang. 1998.)(Xiang-Gen Xia, Jeffrey S. Geronimo, Douglas P. Hardin, and Bruce W. Suter. 1995.), methods of constructing new multifilters (Say Song Goh, Qingtang Jiang, and Tao Xia. 1998.), and methods for application to denoising and compression. Some authors have already presented brief evaluations on the performance of multiwavelets for image compression using orthogonal multiwavelets, and more recently with biorthogonal multiwavelets (Tao Xia and Qingtang Jiang. 1998.). With the very recent work on symmetric signal extension for the class of symmetric-antisymmetric multiwavelets, multiwavelets can now be compared to scalar wavelets on equal footing in practical image compression applications.

The most common entropy coding techniques are run-length encoding (RLE), Huffman coding, arithmetic coding (Glen G. Langdon Jr. 1984.), and Lempel-Ziv (LZ) algorithms. The recent papers in image compression using wavelet transform uses Set Partitioning In Hierarchical Trees Algorithm (SPIHT)(Amir Averbuch, Danny Lazar, and MosheIsraeli. 1996.)(Jerome M. Shapiro. 1993.)(Michael B. Martin, Amy E. Bell, A.A.Beex, Brian D.)(Xiang-Gen Xia, Jeffrey S. Geronimo, Douglas P. Hardin, and Bruce W. Suter. 1995.). The SPIHT algorithm utilizes the structure of scalar wavelet coefficients (Amir Said and William A. Pearlman. 1996.). The multiwavelet coefficient structure is somewhat different from the scalar wavelet coefficients (Michael B. Martin, Amy E. Bell, A.A.Beex, Brian D.). Hence the SPIHT algorithm will not be effective when applying directly on the multiwavelet coefficients. To make it possible some techniques like coefficient shuffling is used (Michael B. Martin and Amy E. Bell. 2001.). New method of making the multiwavelet coefficients fit for the SPIHT algorithm is presented in this paper and the new method results are compared with the coefficient shuffling results.

2. Background

2.1 Multiwavelts

Generalizing the wavelet case, the multiresolution analysis is to be generated by a finite number of scaling functions $\phi_0(t), \phi_1(t), \dots, \phi_{r-1}(t)$ and their integer translates. The multiscaling function $\Phi(t) := [\phi_0(t), \phi_1(t), \dots, \phi_{r-1}(t)]^T$ verifies a 2-scale equation

$$\Phi(t) = 2\sum_{k} M[k]\Phi(2t-k) \tag{1}$$

where $\{M[k]\}_k$ is a finite sequence of $r \times r$ matrices of real coefficients. Construction of an orthonormal basis generated by $\psi_0(t), \psi_1(t), \dots, \psi_{r-1}(t)$ and their integer translates where

$$\Psi(t) \coloneqq \left[\psi_0(t), \psi_1(t), \dots, \psi_{r-1}(t)\right]^T \quad \text{is} \quad \Psi(t) \coloneqq 2\sum_k N[k] \Phi(2t-k)$$
⁽²⁾

with the finite sequence N[k]_k of $r \times r$ matrices of real coefficients coming by completion of $\{M[k]\}_k$.

Introducing the refinement masks $M(z) := \sum_{n} M[n] z^{-n}$ and $N(z) := \sum_{n} N[n] z^{-n}$, the 2-scale equations (1) and (2) translate into fourier domain into

$$\hat{\Phi}(2\omega) = M(e^{j\omega})\hat{\Phi}(\omega) \quad \text{and} \quad \hat{\Psi}(2\omega) \coloneqq N(e^{j\omega})\hat{\Phi}(\omega) \tag{3}$$

The behaviour of the multiscaling function can be derived by iterating the first product above. If this iterated matrix product converge, we get at the limit

$$\hat{\Phi}(\omega) = M_{\infty}(\omega)\hat{\Phi}(0) = \prod_{i=1}^{\infty} M(e^{j\frac{\omega}{2^i}})\hat{\Phi}(0)$$
(4)

By assuming that the scaling functions and their integer translates form an orthogonal basis of V_0 , for $s(t) \in V_0$. Then

$$s(t) = \sum_{n} s_0^{T}[n] \Phi(t-n)$$
(5)

then from $V_0 = V_{-1} \oplus W_{-1}$, we get

$$s(t) = \sum_{n} s_{-1}^{T} [n] \Phi(\frac{t}{2} - n) + d_{-1}^{T} [n] \Psi(\frac{t}{2} - n)$$
(6)

and the well known relations between the coefficients at the analysis step

$$s_{-1}[n] = \sum_{k} M[k - 2n]s_{0}[k]$$
⁽⁷⁾

$$d_{-1}[n] = \sum_{k} N[k - 2n] s_0[k]$$
(8)

and for the synthesis

$$s_0[n] = \sum_k M^T [n - 2k] s_{-1}[k] + N^T [n - 2k] d_{-1}[k]$$
(9)

From these relations, the multi input multi output filter bank can be constructed.

The multiwavelet transform is implemented as a filter bank. A multiwavelet filter bank (G. Strang and V. Strela. 1995.) can be thought of as an M-channel filter bank with filter "taps" that are NxN matrices. The 4 coefficient symmetric multiwavelet filter bank is given in (10). This filter is given by four 2×2 matrices c[k].

$$\begin{bmatrix} d0 & d1 & d2 & d3 \\ d[0] & d[1] & d[2] & d[3] \end{bmatrix} = \frac{1}{10\sqrt{2}} \begin{bmatrix} 6\sqrt{2} & 16 & 6\sqrt{2} & 0 & 0 & 0 & 0 & 0 \\ -1 & -3\sqrt{2} & 9 & 10\sqrt{2} & 9 & -3\sqrt{2} & -1 & 0 \\ -1 & -3\sqrt{2} & 9 & -10\sqrt{2} & 9 & -3\sqrt{2} & -1 & 0 \\ -1 & -3\sqrt{2} & 9 & -10\sqrt{2} & 9 & -3\sqrt{2} & -1 & 0 \\ \sqrt{2} & 6 & -9\sqrt{2} & 0 & 9\sqrt{2} & -6 & -\sqrt{2} & 0 \end{bmatrix}$$
(10)

Each row of the multifilter is a combination of two ordinary filters, one operating on the first data stream and the other operating on the second. The matrix filter coefficients satisfy the orthogonality condition

$$\sum_{k=0}^{N-1} c[k]c[k-2I]^T = 2\delta_{0,I}I$$
(11)

In the time domain, filtering followed by down sampling yields an infinite low pass matrix with "double shifts":

$$L = \begin{bmatrix} \cdots & & & \\ & c[3] & c[2] & c[1] & c[0] & & \\ & & c[3] & c[2] & c[1] & c[0] & & \\ & & & & & \cdots \end{bmatrix}$$
(12)

Each of the filter taps c[k] is a 2×2 matrix. The eigen values of the matrix L are critical for the transition to wavelets – if L has 1 as an eigen value, then there is an associated 2-element vector of scaling functions $\Phi = (\phi_1(t), \phi_2(t))$.

$$\begin{bmatrix} \phi_1(t) \\ \phi_2(t) \end{bmatrix} = \sum_k c[k] \begin{bmatrix} \phi_1(2t-k) \\ \phi_2(2t-k) \end{bmatrix}$$
(13)

The two GHM multiwavelet scaling functions are shown in Figure.1 and the wavelet functions in Figure.2.

Any continuous-time function f(t) in V₀ can be expanded as a linear combination

$$f(t) = \sum v_{1,n}^{(0)} \phi_1(t-n) + v_{2,n}^{(0)} \phi_2(t-n)$$
⁽¹⁴⁾

The superscript (0) denotes an expansion "at scale level 0." f(t) is completely described by the sequences $\begin{cases} 0 \\ V_{1,n} \end{cases} \begin{cases} 0 \\ V_{2,n} \end{cases}$ and their coarse approximation (component in V) is computed with the low pass part of the multiwavelet filter bank ([11]Michael B. Martin and Amy E. Bell. 2001.):

$$\begin{bmatrix} \nu_{1,n}^{(1)} \\ \nu_{2,n}^{(1)} \end{bmatrix} = L \begin{bmatrix} \nu_{1,n}^{(0)} \\ \nu_{2,n}^{(0)} \end{bmatrix}$$
(15)

Analogously, the details $w_{1,n}^{(1)}, w_{2,n}^{(1)}$ in $V_0 \Theta V_1$ are computed with the high pass part d[k].

2.2 Iteration of Decomposition

Since multiwavelet decompositions produce two low pass sub bands and two high pass sub-bands in each dimension, the organization and statistics of multiwavelet sub bands differ from the scalar wavelet case. During a single level of decomposition using a scalar wavelet transform, the 2-D image data is replaced with four blocks corresponding to the subbands.

The multiwavelets used here have two channels, so there will be two sets of scaling coefficients and two sets of wavelet coefficients. Since multiple iterations over the low pass data are desired, the scaling coefficients for the two channels are stored together. Likewise, the wavelet coefficients for the two channels are also stored together. The single level of decomposition for both scalar and multiwavelets are shown in Figure. 3.

Scalar wavelet transforms give a single quarter-sized low pass subband from the original larger subband. The multiwavelet decompositions iterate on the low pass coefficients from the previous decomposition which is shown in Figure.4. In the case of scalar wavelets, the low pass quarter image is a single subband.

But when the multiwavelet transform is used, the quarter images of low pass coefficients is actually a 2×2 block of subbands. Due to the nature of the preprocessing and symmetric extension method, data in these different subbands becomes intermixed during iteration of the multiwavelet transform (V. Strela, P. N. Heller, G. Strang, P. Topiwala, and C. Heil. 1998.).

2.3 SPIHT Algorithm

The SPIHT algorithm was designed and introduced by Said and Pearlman (Amir Said and William A. Pearlman. 1996.). SPIHT exploit the spatial dependence by partitioning the pixel values into parent-descendent groups.

The coder starts with a threshold value that is the largest integer power of two that does not exceed the largest pixel value. Pixels are evaluated in turn to see if they are larger than the threshold; if not, these pixels are considered insignificant. If a parent and all of its descendents are insignificant, then the coder merely records the parent's coordinates. Since the children's coordinates can be inferred from those of the parent, those coordinates are not recorded, resulting in a potentially great savings in the output bit stream. The parent – child relationship in this scheme is shown in Figure 5.

There are three lists maintained in SPIHT encoding. List of significant pixels (LSP), List of insignificant pixels (LIP), and List of insignificant sets (LIS). The descendants of a node include children and grand children. Set of coordinates of all descendants of node (i, j) is denoted as D(i, j). Set of coordinates of four direct offspring of node (i, j) is denoted as O(i, j). Set of coordinates of node (i, j) is denoted as D(i, j) is denoted as L(i, j). After locating and recording all the significant pixels for the given threshold, the threshold is reduced by a factor of two and the process repeats. By the end of each stage, all coefficients that have been found to be significant will have their most significant bits recorded.

3. SPIHT for Multiwavelets

The assumptions that the SPIHT quantizer makes about spatial relations between subbands hold well for scalar wavelets, but they do not hold for multiwavelets. More specifically, the three largest highpass subbands in a scalar wavelet transform are each split into a 2×2block of smaller subbands by the multiwavelet transform, destroying the parent-child relationship that SPIHT presumes. To work around this limitation, there is a method in the thesis of Michael B. Martin (Michael B. Martin and Amy E. Bell. 2001.), referred as coefficient shuffling which presents a new quantization method that allows multiwavelet decompositions to receive most of the benefits of using a quantizer like SPIHT.

3.1 Coefficient Shuffling

The basic idea is to try to restore the spatial features that SPIHT requires for optimal performance. Examination of the coefficients in a single-level multiwavelet transform reveals that there generally exists a large amount of similarity in each of the 2×2 blocks that compose the L_iH_i , H_iL_i and H_iH_i subbands, where i=1, 2 and j=1, 2.

The coefficient shuffling explains the method of rearranging the 2×2 block so that the coefficients corresponding to the same spatial locations are placed together. A clearer picture of this is given in Figure. 6. The remaining coefficient data has the same structure as that of 4-level scalar wavelet decomposition. Solid lines denote new subband boundaries and dashed lines show subband boundaries that are removed by coefficient shuffling.

In this method of coefficient shuffling, the multiwavelet decomposed structure has been altered for implementing SPIHT algorithm. After this process, the spatial relationship of scalar wavelet decomposition is gained in multiwavelet also. Hence, the SPIHT algorithm can be applied for this structure with the usual parent – child relationship. The experimental results using this coefficient shuffling method are giving some better performance over the scalar wavelet

based compression (Michael B. Martin and Amy E. Bell. 2001.). Still it has the performance lack in some type of low frequency images in terms of blocking artifacts.

3.2 Proposed Method

In the coefficient shuffling method, some of the bandpass properties of the coefficients are shuffled with the highpass and lowpass coefficients.

Hence, visual artifacts can be noted in the reconstructed images. In this paper, we propose a new method for making the multiwavelet structure, applicable for SPIHT algorithm without mingling the bandpass coefficients with the highpass coefficients. This process utilizes the conventional multiwavelet decomposition along with the coefficient shuffling.

The horizontal and vertical detail coefficients have their own importance in the reconstruction with same filters used for decomposition. In this method, the decomposition using multiwavelet is done on the entire 2x2 block coefficients of the lowpass filters L_1 and L_2 . i.e. the four subbands L_1L_1, L_1L_2, L_2L_1 and L_2L_2 are considered as approximate coefficients. These four subband coefficients are rearranged and then processed for the second level of decomposition.

The multiwavelet used here is GHM multiwavelet with two scaling and two wavelet functions. There are two lowpass and two highpass filters for decomposition and reconstruction. In each decomposition level, there are four main subbands with their own four subbands as the output of the combination of the filters. Though the coefficient shuffling make the multiwavelet decomposition structure as like the scalar wavelet structure, the combined output of the inner subband coefficients of multiwavelet structure are scattered in the SPIHT encoding. Hence there is large number of blocking artifacts in the reconstructed images, and it is more in natural images (Michael B. Martin and Amy E. Bell. 2001.).

To minimize the artifacts, the shuffling part is avoided for the detailed coefficients in the multiwavelet decomposition. The iteration of decomposition is done until we get the 4x4 matrix as the approximate coefficients. Hence the horizontal, vertical and diagonal details also have the order of 4x4.

At this point, in the approximate 4x4 matrix, the lowest subband element from the filter combination L_1L_1 is considered as the root value without any descendants. Even though the other three coefficients in the same subbands are approximate coefficients, they are considered as detail coefficients for satisfying the SPIHT structure. Then the other three lowest detail subbands are assigned as the children of these three coefficients as like scalar wavelet structure. This is shown in the Figure 8. The dotted lines denote the outputs of the four combinations of the two filters.

In Figure.8, the four coefficients marked by a circle and squares are approximate coefficients of the final level of the decomposition. In this method only one coefficient which is having the highest coefficient value marked by the circle is considered as approximate coefficient and the other three coefficients having the values just less than the highest approximate coefficient are considered as detail coefficients. Here, the actual detail coefficients are assigned as the children of the assumed detail coefficients. Hence the parent child relationship is converted exactly like the scalar wavelet structure. Here the same SPIHT code is applied with these considerations and the results are compared.

4. Experimental Results

Image compression experiments using GHM multiwavelet were conducted in both the coefficient shuffling method and the new method. The results of GHM multiwavelet with coefficient shuffling is denoted by GHM(CS) and the new proposed method is denoted as GHM(N).

Objective results are given in the form of tables of peak signal-to-noise ratio (PSNR) values. Since all tests here are performed on 8-bit grayscale images, the peak signal value is 255. Hence the PSNR values in dB for an M×N image signal x and its reconstruction \hat{x} are calculated via

$$PSNR = 10\log_{10}\left(\frac{255^2}{MSE}\right) \tag{16}$$

where the mean squared error (MSE) is defined as

$$MSE = \frac{1}{MN} \sum_{m=0}^{M-1} \sum_{n=0}^{N-1} |x(m,n) - \hat{x}(m,n)|^2$$
(17)

For each image, three scalar wavelets, a multiwavelet with coefficient shuffling and the new method are tested and the results are compared at different compression ratios. The compression results of different images with different filters are given in the table. The first column gives the image and the second gives wavelet type. The third column gives the PSNR values in dB for that particular image at various compression/bit rates. The bit rates used here correspond to 8-bit grayscale images, so the number of bits per pixel (bpp) is 8 divided by the compression factor. The test results are given for 1.0bpp (8:1), 0.5 bpp (16:1), 0.25 bpp (32:1), or 0.125 bpp (64:1).

The PSNR results for the natural images are given in the Table 1. The natural images contains more low and medium frequency components and also have different type of image structures like straight, curves and surface planes etc. From the results, the new proposed method with GHM multiwavelet outperforms the multiwavelet with coefficient shuffling method in all the cases. It also gives better compression over the scalar wavelets in most of the cases.

The PSNR results for Synthetic images in Table 2 show that the multiwavelets are not that much efficient as the scalar wavelets. Here, for these high frequency components the scalar wavelets are showing very good performance over the multiwavelet methods. Even in some cases, the scalar wavelets are giving lossless compression. Also for the synthetic images for the compression rates considered, the GHM multiwavelet with the new method again giving much better performance than the GHM multiwavelet with the coefficient shuffling method.

5. Conclusion

The performance of multiwavelets in general depends greatly on the image characteristics. For the natural test images, the new method of multiwavelet decomposition and coefficient definition introduced in this paper gives a better performance in many compression rates over the scalar wavelets and the multiwavelet with coefficient shuffling method of encoding. The synthetic images are having more high frequency components. For these types of high frequency images the multiwavelet methods are failed to make over the scalar wavelets. While the shuffling method and the new method present here help standard multiwavelet decompositions work better with zerotree-based quantizers for natural images and synthetic image results are still at a disadvantage. A design of a new multiwavelet with various required mathematical properties could come with a great performance both in natural and synthetic image cases.

References

Amir Averbuch, Danny Lazar, and MosheIsraeli. (Jan 1996). Image Compression Using Wavelet Transform and Multiresolution Decomposition, *IEEE transactions on Image processing*, Vol. 5, No. 1.

Amir Said and William A. Pearlman. (June 1996). A new, fast, and efficient image codec based on set partitioning in hierarchical trees. *IEEE Trans. on Circ. and Syst.* For VideoTech., 6(3): 243–250.

G. Strang and V. Strela, (1995). Short wavelets and matrix dilation equations, IEEE Trans. SP.

Glen G. Langdon Jr. (March 1984). An introduction to arithmetic coding. IBM J. Res. Develop., 28(2):135-149.

Ian H. Witten, Radford M. Neal, and John G. Cleary. (June 1987). Arithmetic coding or data compression. Commications of the ACM, 30(6): 520–540.

Ingrid Daubechies. (1992). Ten Lectures on Wavelets, SIAM, Philadelphia PA, first edition.

ISO/IEC IS 15444-1 / ITU-T Rec. T.800, JPEG 2000 image coding system.

Jerome M. Shapiro. (December 1993). Embedded image coding using zerotrees of wavelet coeffcients. IEEE Trans. on Image Proc., 41(12):3445–3462.

Jo Yew Tham, Li-Xin Shen, Seng Luan Lee, and Hwee Huat Tan. (1998). A general approach for analysis and application of discrete multiwavelet transforms. Preprint.

Michael B. Martin and Amy E. Bell. (April 2001). New image compression techniques using multiwavelets and multiwavelet packets. *IEEE Transactions onImage Processing*, Vol.10, No. 4.

Michael B. Martin, Amy E. Bell, A.A.Beex, Brian D., Applications of multiwavelets to image compression. PG thesis, Blacksburg, Virginia.

Michael Unser, Thierry Blu. (September 2003). Mathematical Propries of the JPEG2000 Wavelet Filters, *IEEE transactions on Image Processing*, Vol. 12, No. 9.

R. C. Calderbank, Ingrid Daubechies, Wim Sweldens, and Boon-Lock Yeo. (1998). Wavelet transforms that map integers to integers. Applied and Computational Harmonic Analysis, 5(3): 332–369.

R. R. Coifman, Y. Meyer, and M. V. Wickerhauser. (1992). Wavelet analysis and signal processing. In Wavelets and their Applications, pages 153–178. Jones and Bartlett, Boston MA.

Say Song Goh, Qingtang Jiang, and Tao Xia. Construction of biorthogonal multiwavelets using the lifting scheme. preprint, 1998.

Tao Xia and Qingtang Jiang. Optimal multifilter banks. (1998). Design, related symmetric extension transform and application to image compression. Preprint.

V. Strela. (1996). Multiwavelets: Theory and Applications. PhD thesis, Massachusetts Institute of Technology.

V. Strela. (1998). A note on construction of biorthogonal multi-scaling functions. Contemporary Mathematics, 216:149–157.

V. Strela and A. T. Walden. (1998). Orthogonal and biorthogonal multiwavelets for signal denoising and image compression. Proc. SPIE, 3391:96–107.

V. Strela, P. N. Heller, G. Strang, P. Topiwala, and C. Heil. (1998). The application of multiwavelet filter banks to image processing. preprint.

Xiang-Gen Xia, Jeffrey S. Geronimo, Douglas P. Hardin, and Bruce W. Suter. (1995). On computations of multiwavelet transforms. Proc. SPIE, 2569:27–38.

Zixiang Xiong, Michael T. Orchard, and Kannan Ramchandran. (1997). A comparative study of DCT and wavelet based coding. Proc. SPIE, 3164: 271 278.

 Table 1. PSNR Results for Natural Test Images

Image	wavelet	1.000 bpp	0.500 bpp	0.250 bpp	0.125 bpp
Mandrill	Haar	31.733	30.603	29.980	29.724
	Db4	32.430	30.852	30.069	29.774
	D:	21.900	20.512	20.040	20,502
	Bior 3.7	31.890	30.513	29.940	29.593
	GHM(N)	42.668	37.223	35.942	31.517
			0,1220		01017
	GHM(CS)	20.419	17.647	16.905	16.460
Boat	Haar	39.211	35.421	33.666	32.565
	Db4	40.902	36.566	34.039	32.481
	D04	40.902	30.300	54.059	52.481
	Bior 3.7	40.159	36.026	33.850	32.393
	GHM(N)	42.969	37.057	36.625	31.326
		a 1 a 4a	10.004	15.000	16026
	GHM(CS) Haar	21.943 38.176	18.334 34.554	17.282 33.392	16.936 32.759
Camera man	IIaai	38.170	34.334	33.372	52.159
	Db4	38.145	34.355	32.798	32.073
	Bior 3.7	37.147	34.117	32.685	31.524
	CID (AD)	10 50 1		21.264	20.007
	GHM(N)	42.724	37.331	31.264	30.987
	GHM(CS)	21.961	18.557	17.621	17.198
Texture	Haar	29.221	28.320	27.856	27.680
	Db4	30.339	29.220	28.413	27.995
	Bior 3.7	30.348	29.170	28.512	28.054
	DI01 5.7	50.546	29.170	20.312	20.034
	GHM(N)	36.728	30.794	25.553	24.374
	GHM(CS)	15.825	13.741	12.574	10.800
Lena	Haar	40.526	36.762	34.715	33.295
	Db4	42.474	39.088	36.202	34.252
	007	72.777	57.000	50.202	57.252
	Bior 3.7	41.448	38.554	35.903	34.070
	GHM(N)	42.782	37.073	36.836	31.483
	CHM(CS)	22 700	10 612	10 224	17 000
	GHM(CS)	22.790	19.613	18.234	17.822

Table 2. PSNR Results for Synthetic Test Images

wavelet	1.000 bpp		0.250 bpp	0.125 bpp
Haar	1.000 bpp ∞	0.500 bpp ∞	0.250 bpp ∞	72.108
Db4	∞	79.961	55.588	47.986
Bior 3.7	∞	99.306	58.167	47.245
GHM(N	48.032	37.096	36.691	31.374
GHM(CS)	25.448	20.471	18.501	17.752
Haar	34.788	32.505	31.409	29.718
Db4	34.299	31.677	30.426	29.532
Bior 3.7	34.962	32.046	30.507	29.520
	25.054	21.102	25.652	25 421
GHM(N)	37.070	31.183	25.652	25.431
CHM(CS)	15 060	13 634	12.853	11.913
· · · · ·				27.762
Tidai	30.072	51.705	27.547	27.702
Db4	30.317	28.788	28.713	27.673
201	001017	201700		271070
Bior 3.7	31.251	31.321	29.170	27.099
GHM(N)	30.805	29.697	25.668	25.393
GHM(CS)	13.074	10.733	8.738	8.074
Haar	44.156	36.925	33.134	31.700
Db4	37.887	33.239	31.473	30.401
Bior 3.7	38.201	33.317	31.374	29.930
	• • • • • •			
GHM(N)	36.890	31.182	29.806	25.186
	15 2 4 2	12.004	10.450	12.045
. ,				12.045 34.103
Пааі	41.108	50.018	54.915	54.105
Db4	41 770	37 205	35 373	33.991
D04	71.//7	57.205	33.373	55.771
Bior 37	39 939	36 562	35 139	34.280
DIGI 3.7	57.757	50.502	55.157	511200
GHM(N)	44.601	39.253	33.964	32.757
(- ·)				
GHM(CS)	35.013	28.963	26.391	25.222
	Db4 Bior 3.7 GHM(N GHM(CS) Haar Db4 Bior 3.7 GHM(N) GHM(CS) Bior 3.7 GHM(N)	Db4 ∞ Bior 3.7 ∞ GHM(N) 48.032 GHM(CS) 25.448 Haar 34.788 Db4 34.299 Bior 3.7 34.962 GHM(N) 37.076 GHM(CS) 15.960 Haar 36.072 Db4 30.317 Bior 3.7 31.251 GHM(N) 30.805 GHM(N) 30.805 GHM(N) 30.805 GHM(N) 30.805 Bior 3.7 38.201 GHM(N) 36.890 GHM(N) 36.890 GHM(N) 36.890 Bior 3.7 38.201 GHM(N) 36.890 GHM(N) 39.939 Bior 3.7 39.939 Bior 3.7 39.939 GHM(N	Db4∞79.961Bior 3.7∞99.306GHM(N48.03237.096GHM(CS)25.44820.471Haar34.78832.505Db434.29931.677Bior 3.734.96232.046GHM(N)37.07631.183GHM(CS)15.96013.634Haar36.07231.703Db430.31728.788Bior 3.731.25131.321GHM(N)30.80529.697GHM(CS)13.07410.733Haar44.15636.925Db437.88733.239Bior 3.738.20133.317GHM(N)36.89031.182GHM(N)36.89031.182GHM(N)36.89031.182GHM(N)36.89031.251Bior 3.738.20133.317GHM(N)36.89031.182Db441.77937.205Bior 3.739.93936.562GHM(N)44.60139.253	Db4∞79.96155.588Bior 3.7∞99.30658.167GHM(N48.03237.09636.691GHM(CS)25.44820.47118.501Haar34.78832.50531.409Db434.29931.67730.426Bior 3.734.96232.04630.507GHM(N)37.07631.18325.652GHM(CS)15.96013.63412.853Haar36.07231.70329.547Db430.31728.78828.713Bior 3.731.25131.32129.170GHM(N)30.80529.69725.668GHM(N)30.80529.69725.668GHM(N)30.80529.69733.134Db437.88733.23931.473Bior 3.738.20133.31731.374GHM(N)36.89031.18229.806GHM(N)36.89031.18229.806GHM(N)36.89031.18229.806GHM(N)36.89031.18229.806GHM(N)36.93936.61834.915Db441.77937.20535.373Bior 3.739.93936.56235.139GHM(N)44.60139.25333.964

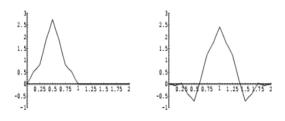


Figure 1. Geronimo-Hardin-Massopust pair of scaling functions

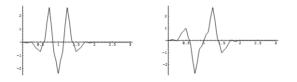


Figure 2. Symmetric GHM pair of wavelet functions

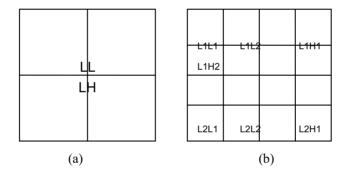


Figure 3. Single level decomposition structure for (a) scalar wavelets and (b) multiwavelets

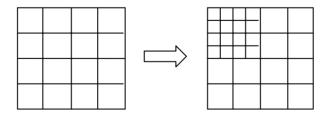


Figure 4. Iteration of multiwavelet decomposition.

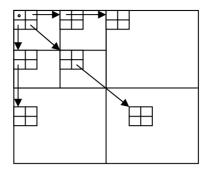


Figure 5. Illustration of parent-child relationship

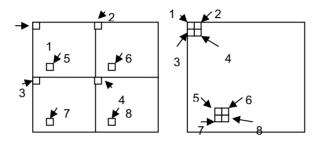


Figure 6. Illustration of coefficient shuffling

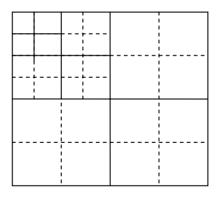


Figure 7. Subbands in 2-level multiwavelet decomposition after coefficient shuffling

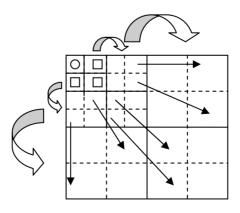


Figure 8. Parent - child relationship of multiwavelet decomposed structure